# 

# (11) EP 4 394 064 A1

(12)

# **EUROPEAN PATENT APPLICATION**

published in accordance with Art. 153(4) EPC

(43) Date of publication: 03.07.2024 Bulletin 2024/27

(21) Application number: 23866641.6

(22) Date of filing: 01.09.2023

(51) International Patent Classification (IPC):

C22C 9/00 (2006.01) C22C 9/10 (2006.01)

C22F 1/00 (2006.01) C22F 1/08 (2006.01)

(52) Cooperative Patent Classification (CPC): C22C 9/00; C22C 9/10; C22F 1/00; C22F 1/08

(86) International application number: **PCT/JP2023/032138** 

(87) International publication number: WO 2024/090037 (02.05.2024 Gazette 2024/18)

(84) Designated Contracting States:

AL AT BE BG CH CY CZ DE DK EE ES FI FR GB GR HR HU IE IS IT LI LT LU LV MC ME MK MT NL NO PL PT RO RS SE SI SK SM TR

Designated Extension States:

BA

**Designated Validation States:** 

KH MA MD TN

(30) Priority: 28.10.2022 JP 2022173377

(71) Applicant: NGK INSULATORS, LTD. Nagoya-shi, Aichi 4678530 (JP)

(72) Inventors:

 UCHIYAMA Hiromitsu Nagoya-shi, Aichi 4678530 (JP)

 CHIBA Koki Nagoya-shi, Aichi 4678530 (JP)

(74) Representative: Mewburn Ellis LLP
Aurora Building
Counterslip
Bristol BS1 6BX (GB)

# (54) LEAD-FREE FREE-CUTTING BERYLLIUM COPPER ALLOY

(57) There is provided a lead-free free-cutting beryllium copper alloy that is superior in machinability. The lead-free free-cutting beryllium copper alloy consists of from 1.80% to 2.10% by weight of Be, from 0.10% to 3.00% by weight of Si, from 0.20% to 0.40% by weight of Co, from 0% to 0.10% by weight of Fe, from 0% to

0.10% by weight of Ni, and the balance being Cu and inevitable impurities, wherein the beryllium copper alloy includes a matrix phase being an  $\alpha$  phase, a Si-rich phase being a  $\kappa$  phase rich in Si, and Co-Be-Si intermetallic compound grains containing Co, Be, and Si, and optionally Fe and/or Ni.

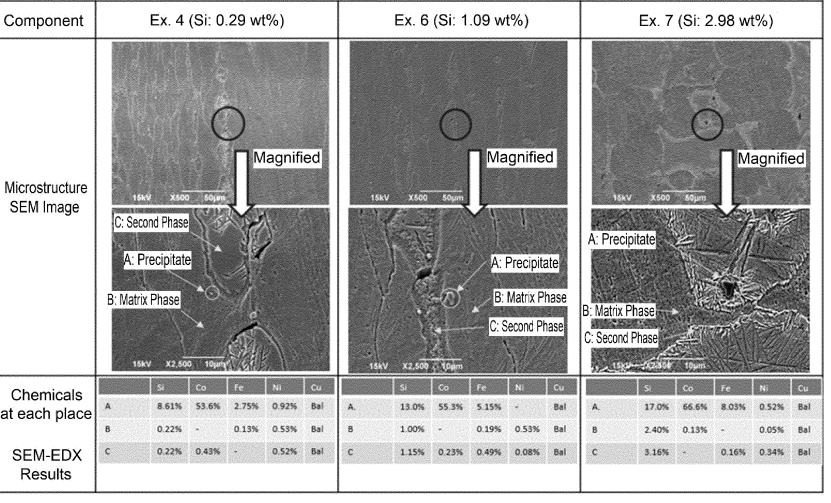


FIG. 1

#### Description

10

20

25

35

50

55

#### **TECHNICAL FIELD**

<sup>5</sup> **[0001]** The present invention relates to a lead-free free-cutting beryllium copper alloy.

#### **BACKGROUND ART**

**[0002]** Beryllium copper alloys have traditionally been widely used in electronic components such as connectors because of their high strength and high electrical conductivity. Patent Literature 1 (JPS50-139017A) discloses a quaternary copper alloy for spring materials, composed of from 0.5% to 1.5% of Be, from 0.2% to 3.0% of Sn, from 0.5% to 2.0% of Si, and the balance being Cu and inevitable impurities as an example of beryllium copper alloys.

**[0003]** Among beryllium copper alloys, a free-cutting beryllium copper alloy (UNS No.: C17300) is generally known as a beryllium copper alloy with superior machinability. This alloy is improved in machinability by allowing beryllium copper to contain from about 0.2% to 0.6% by weight of lead (Pb). For example, Patent Literature 2 (JPS54-30369B) discloses a free-cutting beryllium copper alloy as such a copper alloy, in which a copper alloy containing 0.5% to 4% by weight of Be is allowed to contain from 0.01% to 3% by weight of one selected from Pb, Te, and Bi, from 0.01% to 5% by weight of rare earth elements, and from 0.1% to 5% by weight of Al or Si.

**[0004]** Also, free-cutting brass using brass materials has been developed, as well as beryllium copper alloys. For example, Patent Literature 3 (JP2000-119775A) discloses a leadless free-cutting copper alloy defined by an alloy composition composed of from 69% to 79% by weight of Cu, from 2.0% to 4.0% by weight of Si, and the balance consisting of Zn. Also, Patent Literature 4 (JP2021-42459A) discloses a free-cutting copper alloy containing from 58.5 mass% to 63.5 mass% of Cu, from more than 0.4 mass% to 1.0 mass% of Si, from 0.003 mass% to 0.25 mass% of Pb, from 0.005 mass% to 0.19 mass% of P, and the balance composed of Zn and inevitable impurities.

CITATION LIST

#### PATENT LITERATURE

#### 30 [0005]

Patent Literature 1: JPS50-139017A Patent Literature 2: JPS54-30369B Patent Literature 3: JP2000-119775A Patent Literature 4: JP2021-42459A

# SUMMARY OF INVENTION

[0006] Lead-containing copper alloys, including free-cutting beryllium copper alloys as disclosed in Patent Literature 2, are superior in machinability, as described above, and accordingly have been conventionally used as a constituent material of various products. However, lead is a harmful substance that adversely affects the human body and environment, and its use has tended to be greatly restricted in recent years. Accordingly, in brass materials, lead-free free-cutting brass has been developed, as disclosed in Patent Literatures 3 and 4. For beryllium copper alloys, however, there is no practical free-cutting material free from lead, and lead-free free-cutting beryllium copper alloys have been long awaited to be developed.

**[0007]** The present inventors have recently found that a specific microstructure formed by allowing a beryllium copper alloy containing from 1.80% to 2.10% by weight of Be to contain from 0.10% to 3.00% by weight of Si can provide a lead-free beryllium copper alloy exhibiting superior machinability.

**[0008]** Accordingly, an object of the present invention is to provide a lead-free free-cutting beryllium copper alloy that is superior in machinability.

[0009] The present invention provides the following aspects:

[Aspect 1]

A lead-free free-cutting beryllium copper alloy, consisting of:

from 1.80% to 2.10% by weight of Be; from 0.10% to 3.00% by weight of Si; from 0.20% to 0.40% by weight of Co;

from 0% to 0.10% by weight of Fe; from 0% to 0.10% by weight of Ni; and the balance being Cu and inevitable impurities, wherein the beryllium copper alloy has:

5

15

20

25

35

40

50

55

a matrix phase being an  $\alpha$  phase,

a Si-rich phase being a  $\kappa$  phase rich in Si, and

Co-Be-Si intermetallic compound grains containing Co, Be, and Si, and optionally Fe and/or Ni.

[Aspect 2] The lead-free free-cutting beryllium copper alloy according to aspect 1, wherein the Co-Be-Si intermetallic compound grains exhibit a hardness from 1.0 to 12.0 GPa as measured by a nanoindentation test in accordance with ISO14577.

[Aspect 3] The lead-free free-cutting beryllium copper alloy according to aspect 1 or 2, wherein the number of the Co-Be-Si intermetallic compound grains present at a cross section of the lead-free free-cutting beryllium copper alloy is 320 or less per unit area of 1 mm<sup>2</sup>.

[Aspect 4] The lead-free free-cutting beryllium copper alloy according to any one of aspects 1 to 3, wherein when a cross section of the lead-free free-cutting beryllium copper alloy is observed, the Co-Be-Si intermetallic compound grains have a cross-sectional area from 0.3 to 70  $\mu$ m<sup>2</sup> per grain.

[Aspect 5] The lead-free free-cutting beryllium copper alloy according to any one of aspects 1 to 4, wherein when a cross section of swarf generated by cutting the lead-free free-cutting beryllium copper alloy is observed along a longitudinal direction, the cross section of the swarf has a sheared profile with zigzag-shaped unevenness that satisfies a relationship  $1.10 < h_2/h_1 < 6.60$ , wherein  $h_1$  represents the average of distances between recesses in the zigzag-shaped unevenness, and  $h_2$  represents the average of heights of protrusions in the unevenness.

[Aspect 6] The lead-free free-cutting beryllium copper alloy according to any one of aspects 1 to 5, wherein in a phase map of 75  $\mu$ m  $\times$  75  $\mu$ m field of view obtained by electron beam backscatter diffraction (EBSD) analysis of a cross section of the lead-free free-cutting beryllium copper alloy, the percentage of area  $S_{BCC}$  of BCC regions identified as body-centered cubic (BCC) lattices relative to the sum of area  $S_{FCC}$  of FCC regions identified as face-centered cubic (FCC) lattices and area  $S_{BCC}$ , that is,  $100 \times S_{BCC}/(S_{FCC} + S_{BCC})$ , is 5% or more.

## 30 BRIEF DESCRIPTION OF DRAWINGS

## [0010]

Figure 1 depicts sectional SEM images and SEM-EDX results of copper alloy samples of Examples 4, 6, and 7. Figure 2A depicts sectional SEM images of the copper alloy sample (Si: 1.09% by weight) of Example 6 at varying magnifications.

Figure 2B depicts EPMA mapping images of Example 6 measured in the region corresponding to the SEM image in the lower right of Figure 2A.

Figure 3A depicts sectional SEM images of the copper alloy sample (Si: 2.98% by weight) of Example 7 at varying magnifications.

Figure 3B depicts EPMA mapping images of Example 7 measured in the region corresponding to the SEM image in the lower right of Figure 3A.

Figure 3C depicts EPMA mapping images of Example 7 measured in the region corresponding to the SEM image in the lower right of Figure 3A.

Figure 4A depicts sectional STEM images of the copper alloy sample (Si: 1.09% by weight) of Example 6 at varying magnifications.

Figure 4B depicts STEM-EELS mapping images of Example 6 measured in the region corresponding to the STEM image at the right end of Figure 4A.

Figure 5A depicts a CCD image of the copper alloy sample (Si: 0.29% by weight) of Example 4 and the hardness distribution in the rectangular region of the CCD image.

Figure 5B depicts a histogram of the hardness distribution of intermetallic compound grains measured for the copper alloy sample (Si: 0.29% by weight) of Example 4.

Figure 6 depicts a sectional SEM image of the copper alloy sample (Si: 2.98% by weight) of Example 7.

Figure 7 depicts schematic diagrams illustrating the method of cutting a copper alloy sample in machinability evaluation 1 for the Examples.

Figure 8A depicts SEM images in observing cross sections of swarf from copper alloy samples in Examples 2 to 4. Figure 8B depicts SEM images in observing cross sections of swarf from copper alloy samples in Examples 5 to 7. Figure 9 depicts a schematic diagram illustrating distance  $h_1$  between recesses and the largest height  $h_2$  of the

protrusions in the unevenness at a cross section of swarf in machinability evaluation 1 for the Examples.

Figure 10 depicts a schematic diagram illustrating the method of cutting a copper alloy sample in machinability evaluation 2 for the Examples.

Figure 11 depicts Table 2 presenting sectional SEM images of copper alloy samples of Examples 1 and 5 to 7 and EBSD phase maps of the regions corresponding to the respective sectional SEM images, each together with the area percentage of the BCC region and the cutting resistance (thrust force).

#### **DESCRIPTION OF EMBODIMENTS**

5

15

20

30

35

40

45

50

# Lead-Free Free-Cutting Beryllium Copper Alloy

[0011] The lead-free free-cutting beryllium copper alloy according to the present invention consists of from 1.80% to 2.10% by weight of Be, from 0.10% to 3.00% by weight of Si, from 0.20% to 0.40% by weight of Co, from 0% to 0.10% by weight of Fe, from 0% to 0.10% by weight of Ni, and the balance being Cu and inevitable impurities. Needless to say, lead-free free-cutting beryllium copper alloy contains no lead (Pb). This copper alloy has a matrix phase being an  $\alpha$  phase, a Si-rich phase being a  $\kappa$  phase rich in Si, and Co-Be-Si intermetallic compound grains. The Co-Be-Si intermetallic compound grains contain Co, Be, and Si, and optionally Fe and/or Ni. Thus, a specific microstructure formed by allowing a beryllium copper alloy containing from 1.80% to 2.10% by weight of Be to contain from 0.10% to 3.00% by weight of Si can provide a lead-free beryllium copper alloy exhibiting superior machinability.

[0012] Lead-containing copper alloys, including free-cutting beryllium copper alloys, are superior in machinability, as described above, and accordingly have been conventionally used as a constituent material of various products. However, lead is a harmful substance that adversely affects the human body and environment, and its use has tended to be greatly restricted in recent years. For beryllium copper alloys, it is an issue that there is no practical lead-free free-cutting material. In this regard, the lead-free free-cutting beryllium copper alloy of the present invention can solve the above issue favorably. More specifically, allowing a beryllium copper alloy to contain Si reduces the cutting resistance of the beryllium copper alloy. Also, the swarf produced by cutting beryllium copper alloys containing Si is easy to shear into chips and unlikely to wind around the tool. Thus, the beryllium copper alloy of the present invention exhibits superior machinability not only in terms of reducing cutting resistance but also in terms of improving the shapes of the swarf. Note that "lead-free" in the lead-free free-cutting beryllium copper alloy means that the lead content is lower than or equal to the detection limit in the elemental analysis of the copper alloy.

**[0013]** Although the mechanism by which the presence of Si (particularly, the presence of Si-rich phases and Co-Be-Si intermetallic compound grains) improves the machinability is not clear, the Si-rich phases and Co-Be-Si intermetallic compound grains containing Si probably serve as a stress concentration origin of shear failure to facilitate the braking of the swarf into smaller pieces.

**[0014]** Be imparts superior fundamental performance (strength, workability, fatigue properties, heat resistance, corrosion resistance, etc.) as beryllium copper alloy to copper alloy. The Be content of the copper alloy of the present invention is from 1.80% to 2.10% by weight and is preferably from 1.80% to 2.00% by weight. A Be content in such a range can lead to the above-mentioned fundamental performance effectively and prevent excess Be from reducing electric conductivity.

[0015] Si forms Si-rich phases and Co-Be-Si intermetallic compound grains to impart superior machinability to beryllium copper alloy. The Si content of the copper alloy of the present invention is from 0.10% to 3.00% by weight, preferably from 0.30% to 2.50% by weight, more preferably from 0.45% to 2.50% by weight, still more preferably from 0.50% to 2.20% by weight, particularly preferably from 0.80% to 2.00% by weight and is, for example, from 1.00% to 2.00% by weight. A Si content in such a range can improve machinability effectively and prevent excess Si from reducing productivity (causing cracking during forging) in actual operations. Particularly when the Si content is 0.45% by weight or more, Sirich phases increase with statistical significance, and their remarkable shear occurs during cutting, further improving machinability. Accordingly, the Si content of the copper alloy can be preferably from 0.45% to 3.00% by weight, more preferably from 0.50% to 3.00% by weight, particularly preferably from 1.00% to 3.00% by weight, for example, from 2.00% to 3.00% by weight.

**[0016]** Co forms Co-Be-Si intermetallic compound grains to impart superior machinability to beryllium copper alloy. The Co content of the copper alloy of the present invention is from 0.20% to 0.40% by weight, preferably from 0.20% to 0.35% by weight, more preferably from 0.22% to 0.30% by weight, and particularly preferably from 0.22% to 0.28% by weight. A Co content in such a range enables effective crystal refinement and the improvement of copper alloy properties and can prevent excess Co from reducing productivity in actual operations.

[0017] Fe and Ni are optional elements that may be considered as impurities in the copper alloy of the present invention, and desired to be as little as possible because high Fe and Ni contents degrade mechanical properties. Accordingly, the Fe and Ni contents of the copper alloy of the present invention are each from 0% to 0.10% by weight, preferably from 0% to 0.005% by weight.

**[0018]** As described above, the copper alloy of the present invention has a microstructure including a matrix phase, Si-rich phases, and Co-Be-Si intermetallic compound grains. Typically, the Si-rich phases are present in the matrix phase, and the Co-Be-Si intermetallic compound grains are present at the interfaces between the Si-rich phases and the matrix phase.

**[0019]** The matrix phase is defined by an  $\alpha$  phase and contributes to the superior fundamental performance (strength, workability, fatigue properties, heat resistance, corrosion resistance, etc.) as beryllium copper alloy.

**[0020]** A Si-rich phase is defined by a  $\kappa$  phase rich in Si and contributes to improving the machinability. In particular, the presence of Si in the matrix phase improves shearability and facilitates breaking the swarf into smaller pieces. The expression "rich in Si" means that Si is detected in a higher concentration in the elemental analysis than in the matrix phase ( $\alpha$  phase) and not necessarily in a higher concentration than in Co-Be-Si intermetallic compound grains.

[0021] Typically, the matrix phase has a face-centered cubic (FCC) lattice crystal structure, while the Si-rich phase has a body-centered cubic (BCC) lattice crystal structure. The BCC structure is unlikely to deform and more shearable than the FCC structure. This means that Si-rich phases having a BCC structure can also contribute to improving the machinability. Accordingly, in a phase map of 75  $\mu m \times 75 \ \mu m$  field of view obtained by electron beam backscatter diffraction (EBSD) analysis of a cross section of the beryllium copper alloy, the percentage of area  $S_{BCC}$  of BCC regions identified as body-centered cubic (BCC) lattices relative to the sum of area  $S_{FCC}$  of FCC regions identified as face-centered cubic (FCC) lattices and area  $S_{BCC}$  of BCC regions (that is,  $100 \times S_{BCC}$  / ( $S_{FCC} + S_{BCC}$ )) is preferably 5% or more, more preferably from 5 to 40%, still more preferably from 10 to 30%, particularly preferably from 15 to 30%, and most preferably from 15 to 25%. By increasing the percentage of such a BCC structure, the cutting resistance (particularly thrust force) can be reduced, resulting in further improved machinability. The EBSD measurement can be conducted according to the procedure and conditions described in the Examples below.

**[0022]** Co-Be-Si intermetallic compound grains also contribute to improving the machinability. The Co-Be-Si intermetallic compound grains contain Co, Be, and Si, and optionally Fe and/or Ni. Hence, Co-Be-Si intermetallic compound grains contain Co, Be, and Si as essential elements, and these elements are dominant. Fe and Ni are optional elements or trace elements that can be considered impurities, as mentioned above and are, therefore, not considered dominant in the Co-Be-Si intermetallic compound grains.

[0023] The Co-Be-Si intermetallic compound grains preferably have a hardness from 1.0 to 12.0 GPa, more preferably from 1.5 to 7.5 GPa, and still more preferably from 2.0 to 6.0 GPa as measured by a nanoindentation test in accordance with ISO14577. Having a hardness in such a range achieves machinability effectively. The nanoindentation test measures hardness in a small region at many points, and the resulting hardnesses have a wide distribution. Therefore, 100% of the measured points of the Co-Be-Si intermetallic compound grains need not be within the above ranges as long as the majority (for example, 90% or more) is within the above ranges. Hence, it is acceptable that the distribution of measured hardnesses includes hardnesses less than 1.0 GPa or higher than 12.0 GPa to a small extent (for example, less than 10%). [0024] The number of Co-Be-Si intermetallic compound grains is not limited, provided that the machinability of the beryllium copper alloy can be improved without impairing the above-described fundamental performance. From the viewpoint of improving machinability more effectively, the number of Co-Be-Si intermetallic compound grains at a cross section of the copper alloy is preferably 320 or less per unit area of 1 mm², more preferably from 50 to 300, and still more preferably from 80 to 200.

[0025] The shape of Co-Be-Si intermetallic compound grains is not limited to spherical and may be plate-like, rod-shaped, needle-shaped, or in variant shapes without limitation. Accordingly, the size of the Co-Be-Si intermetallic compound grains is preferably specified by cross-sectional area rather than by diameter. For example, in the cross section of the beryllium copper alloy, the Co-Be-Si intermetallic compound grains have a cross-sectional area preferably from 0.3 to 70  $\mu$ m<sup>2</sup> per grain, more preferably from 1.0 to 65  $\mu$ m<sup>2</sup>, and still more preferably from 5.0 to 60  $\mu$ m<sup>2</sup>.

**[0026]** The copper alloy of the present invention has superior machinability, as described above, and when a cross section of the swarf generated by cutting the copper alloy is observed along a longitudinal direction, the cross section of the swarf has a sheared profile with zigzag-shaped unevenness. In this instance, the zigzag-shaped unevenness preferably satisfies the relationship  $1.10 < h_2/h_1 < 6.60$ , more preferably  $2.0 < h_2/h_1 < 6.6$ , and still more preferably  $2.5 < h_2/h_1 < 6.6$ , wherein as depicted in Figures 8,  $h_1$  represents the average of distances between recesses in the zigzag-shaped unevenness, and  $h_2$  represents the average of heights of the protrusions in the unevenness. When the swarf produced by cutting the copper alloy has such a sheared profile, the swarf is easy to shear into chips and unlikely to wind around the tool. Such copper alloy can be superior in machinability. In contrast, when the swarf has an undulatory profile (smoothly uneven profile) rather than a sheared profile, the swarf easily forms strings of cut pieces, which are likely to wind around the tool, reducing productivity.

### Production Method

10

15

30

35

50

55

**[0027]** The lead-free free-cutting beryllium copper alloy of the present invention can be preferably produced by, but not limited to, (a) melting and casting of raw materials for the above-described composition; (b) homogenization heat

treatment; (c) hot working; (d) cold working; (e) solution annealing; and (f) aging treatment, in this order. The preferred aspects of copper alloys have been described above, and thus descriptions will be omitted here.

(a) Melting and Casting

5

10

20

35

40

50

55

**[0028]** First, one or more raw materials whose constituents are adjusted to result in the above-described composition (that is, composition consisting of from 1.80% to 2.10% by weight of Be, from 0.10% to 3.00% by weight of Si, from 0.20% to 0.40% by weight of Co, from 0% to 0.10% by weight of Fe, from 0% to 0.10% by weight of Ni, and the balance being Cu and inevitable impurities) are melted into a copper alloy molten metal. If a given element is added, the element alone, a master alloy, or the like can be added to the raw material. Alternatively, a raw material containing such additive elements may be melted together with a copper raw material. Then, the copper alloy molten metal whose constituents are adjusted to result in the above-described composition is poured into a mold to form an ingot. For mass production, continuous casting is preferred. Thus, a (cylindrical, for example) ingot (billet) can be produced.

(b) Homogenization Heat Treatment

**[0029]** The resulting ingot is subjected to homogenization heat treatment. That is, the ingot is homogenized by heating. In homogenization heat treatment, the heating temperature of the ingot is preferably in the range of 500 to 900°C, and the temperature is preferably held in this range for a period from 1 to 24 hours.

(c) Hot Working

**[0030]** The ingot subjected to homogenization heat treatment is hot-worked into a hot-worked material with a predetermined diameter. Before hot working, the homogenized ingot may be optionally annealed for softening to improve workability. Although, at this time, annealing conditions are not limited, the heating temperature is preferably in the range from 500 to 900°C, and the temperature is preferably held in this range for a period from 0.2 to 6 hours.

(d) Cold Working

[0031] The resulting hot-worked material is cold-worked into a cold-worked material with a predetermined diameter. The cold working percentage is preferably from 0.5 to 95%. Before cold working, the hot-worked material may be optionally annealed for softening to improve workability. Although, at this time, annealing conditions are not limited, the heating temperature is preferably in the range from 500 to 900°C, and the temperature is preferably held in this range for a period from 0.2 to 6 hours.

(e) Solution Annealing

**[0032]** The resulting cold-worked material is subjected to solution annealing to uniformly dissolve the elements in the material, yielding a solution-annealed material. In the solution annealing, the solution annealing temperature is preferably in the range from 600 to 900°C, and the temperature is preferably held in this range for a period from 0.2 to 3 hours.

(f) Aging Treatment

**[0033]** The resulting solution-annealed material is subjected to aging treatment to obtain the beryllium copper alloy of the present invention. In the aging treatment, the aging temperature is preferably in the range from 200 to 500°C, and the temperature is preferably held in this range for a period from 0.2 to 3 hours. Before aging treatment, the solution-annealed material may be optionally subjected to cold working or oxide coating removal. At this time, the cold working conditions are not limited, but the working percentage is preferably from 0.5 to 95%.

**[0034]** The lead-free beryllium copper alloy with superior machinability can be favorably produced through the above steps (a) to (f).

**EXAM PLES** 

[0035] The present invention will be further described in detail with reference to the following Examples.

Examples 1 to 7

[0036] Beryllium copper alloys were produced according to the following procedure and evaluated.

(1) Melting and Casting

**[0037]** First, a copper alloy raw material that can provide the compositions presented in Table 1 was prepared. The copper alloy raw material was melted, and the resulting molten metal was poured into a mold to form a cylindrical ingot (billet).

(2) Homogenization Heat Treatment

[0038] The resulting ingot was held at 800°C for 4 hours for homogenization heat treatment.

(3) Hot Working

5

10

15

20

25

30

35

40

50

55

[0039] The ingot subjected to homogenization heat treatment was annealed at 800°C for 1 hour and then hot-worked into a cylindrical hot-worked material with a diameter of 1.8 cm.

(4) Cold Working

**[0040]** Before hot-working into a hot-worked material, the material was annealed at 800°C for 1 hour and then subjected to cold-working at a working percentage of 40% into a cylindrical cold-worked material with a diameter of 1.4 cm.

(5) Solution Annealing

[0041] The resulting cold-worked material was subjected to solution annealing at 800°C for 1 hour to yield a solution-annealed material.

(6) Aging Treatment

**[0042]** The solution-annealed material was cold-worked at a working percentage of 38%. The resulting solution-annealed material was subjected to aging treatment at 320°C for 2 hours to yield a cylindrical beryllium copper alloy sample with a diameter of 1.1 cm and a length of 100 cm.

(7) Evaluation

[0043] The resulting beryllium copper alloy sample (hereinafter referred to as a copper alloy sample) was evaluated in terms of the following.

<SEM-EDX and EPMA>

[0044] The copper alloy sample was cut into a cross section and sliced with a focused ion beam (FIB). The resulting cross section was observed under an SEM (scanning electron microscope), and the cross section was subjected to elemental analysis under the measurement condition of an accelerating voltage of 15 kV with an energy dispersive X-ray analyzer (EDX, model name: JXA-8530FPlus, manufactured by JEOL Ltd.) attached to the SEM. The same cross section was also subjected to elemental analysis under the measurement condition of an accelerating voltage of 15 kV with an electron probe microanalyzer (EPMA, model name: JXA-8530FPlus, manufactured by JEOL Ltd.)

[0045] The results showed that the beryllium copper alloys of Examples 3 to 7 include the matrix phase, Si-rich phases containing a higher concentration of Si than the matrix phase, and Co-Be-Si intermetallic compound grains containing Co, Be, Si, Fe, and Ni. It was also identified that Co-Be-Si intermetallic compound grains contain a still higher concentration of Si than the Si-rich phases. Figure 1 depicts SEM images of the samples of Examples 4, 6, and 7 and their SEM-EDX results at individual measurementlocations.

**[0046]** Figure 2A depicts sectional SEM images of the copper alloy sample (Si: 1.09% by weight) of Example 6 at varying magnifications. In Figure 2A, the three SEM images on the left are secondary electron micrographs, clearly showing fine structures at a surface of the sample, and the three SEM images on the right are backscattered electron composition images (COMPO images), showing contrasts dependent on the atomic numbers. Any of these six SEM images are obtained by observing the same face of the sample. Figure 2B depicts EPMA mapping images of Example 6 measured in the region corresponding to the SEM image in the lower right of Figure 2A.

[0047] Similarly, Figure 3A depicts sectional SEM images of the copper alloy sample (Si: 2.98% by weight) of Example 7 at varying magnifications. In Figure 3A, the three SEM images on the left are secondary electron micrographs, clearly showing fine structures at a surface of the sample, and the three SEM images on the right are backscattered electron

composition images (COMPO images), showing contrasts dependent on the atomic numbers. Any of these six SEM images are obtained by observing the same face of the sample. Figures 3B and 3C depict EPMA mapping images of Example 7 measured in the region corresponding to the SEM image in the lower right of Figure 3A.

<STEM-EELS>

5

10

20

30

35

45

50

55

[0048] The copper alloy sample was cut into a cross section and sliced with a focused ion beam (FIB). The resulting cross section was observed under the measurement condition at an accelerating voltage of 200 kV under a scanning transmission electron microscope with a spherical aberration correction function (STEM, model name: HD-2700, manufactured by Hitachi High-Tech Corporation). Additionally, elemental analysis was performed on the vicinity of interfaces between the matrix phase and the intermetallic compound grains under the measurement condition of 200 kV voltage with an electron energy loss spectrometer (EELS, trade name: Enfinium, manufactured by Gatan Inc.) / energy dispersive X-ray analyzer (EDX, model name: XMAXN 100TLE, manufactured by Oxford Instruments plc) attached to the STEM. The results showed that the intermetallic compound grains in the beryllium copper alloys of Examples 3 to 7 were dominated by Co, Be, and Si, with Ni and Fe merely in trace amounts. Hence, the presence of Co-Be-Si intermetallic compound grains was confirmed. Also, it was identified that the matrix phase contains mainly Be and Cu, in which Cu is dominant. Furthermore,  $\alpha$  phases in the matrix phase and  $\kappa$  phases in the Si-rich phases were identified. Figure 4A depicts sectional STEM images of the copper alloy sample (Si: 1.09% by weight) of Example 6 at varying magnifications, and Figure 4B depicts STEM-EELS mapping images of Example 6 measured in the region corresponding to the STEM image in the right end of Figure 4A.

<Hardness of Intermetallic Compound Grains>

[0049] The hardness (GPa) of Co-Be-Si intermetallic compound grains at the cross section of beryllium copper alloys was measured at each microregion by a nanoindentation test. This test was performed in accordance with ISO14577 on samples with a Poisson's ratio of 0.3 under the conditions of 0.25 mN maximum load,  $60~\mu m$  (X axis)  $\times$   $60~\mu m$  (Y axis) measurement region, and  $60~(X~axis) \times 60~(Y~axis)$  measurement points using a nanoindenter (trade name: iMicro nanoindenter, manufactured by KLA Corporation). The hardness distribution of the Co-Be-Si intermetallic compound grains thus measured were represented by histograms. The results showed that the Co-Be-Si intermetallic compound grains in the samples of Examples 4, 6, and 7 have hardnesses from 1.0 to 12.0 GPa, as presented in Table 1. Figure 5A depicts a CCD image of the copper alloy sample (Si: 0.29% by weight) of Example 4 and the hardness distribution in the rectangular region of the CCD image, and Figure 5B depicts a histogram of the hardness distribution thus obtained.

<Number of Intermetallic Compound Grains>

[0050] The cross sections of copper alloy samples were observed by SEM at a magnification of 500 times to obtain sectional SEM images in a field of view of 48118.52  $\mu$ m<sup>2</sup>. The number of Co-Be-Si intermetallic compound grains was counted in the field of view with this area and converted into a number per unit area of 1 mm<sup>2</sup>. Thus, the number of Co-Be-Si intermetallic compound grains present at a cross section of the beryllium copper alloy was obtained per unit area of 1 mm<sup>2</sup>. The results are presented in Table 1. Figure 6 depicts a sectional SEM image (area of field of view: 48118.52  $\mu$ m<sup>2</sup>) of the copper alloy sample (Si: 2.98% by weight) of Example 7. In Figure 6, black dots represent Co-Be-Si intermetallic compound grains, and the number of the dots was 15. Thus, the number of Co-Be-Si intermetallic compound grains present at a cross section was identified as 311 per unit area of 1 mm<sup>2</sup>.

<Area of Intermetallic Compound Grains>

**[0051]** Cross sections of copper alloy samples were observed at a magnification from 1000 to 2500 times by SEM, and the area  $(\mu m^2)$  per grain of Co-Be-Si intermetallic compound grains in the respective beryllium copper alloys was calculated. The results are presented in Table 1.

<Machinability Evaluation 1 (h<sub>2</sub>/h<sub>1</sub> and Swarf Shape)>

**[0052]** Copper alloy samples were used as work materials to be cut, and the swarf produced when the work materials were cut with a tool (tool bit) was examined. More specifically, as illustrated in Figure 7, a work material 2 was moved in a straight line, and the surface layer at the top of the work material was cut with a tool 4 (as in planing). At this time, the copper alloy was cut under the conditions of 150 m/min cutting speed, a cutting position at a depth of 0.10 mm from the copper alloy surface and 2 mm cutting width, and 5° rake angle. The profile of the cross section of swarf was identified by observing the copper alloy sample at a magnification of 200 times by SEM. The results are presented in Table 1.

Figures 8A and 8B depict SEM images at cross sections of the swarf obtained at this time, observed in Examples 2 to 7. The cross section of the swarf desirably has a sheared profile with zigzag-shaped unevenness. This is because when the swarf produced by cutting the copper alloy has such a sheared profile, the swarf is easy to shear into chips and unlikely to wind around the tool. In contrast, when the swarf has an undulatory profile (smoothly uneven profile) rather than a sheared profile, the swarf easily forms strings of cut pieces, which are likely to wind around the tool, reducing productivity. Then, distances between the recesses in the unevenness of the swarf were measured, and their average  $h_1$  was calculated, as depicted in Figure 9. Also, the heights of the protrusions in the unevenness were measured, and their average  $h_2$  was calculated. Figures 8A and 8B retain auxiliary lines drawn at this time by hand to calculate the distances. The resulting average  $h_2$  was divided by average  $h_1$  to obtain ratio  $h_2/h_1$  (degree of unevenness). The results are presented in Table 1. For Examples 1 and 5 to 7, when the sample was cut, the thrust force, which is one of the partial forces constituting the cutting resistance, was measured as an indicator of the cutting resistance of the work material by a three-component force dynamometer (Type 9601A32, manufactured by Kistler Group). Thus, values presented in Table 2 (see Figure 11) were obtained.

15 <Machinability Evaluation 2 (Cutting Resistance)>

[0053] Copper alloy samples were used as work materials, and the cutting resistance (N) of the work materials when cut with a tool (tool bit) was examined. More specifically, a work material 2 was lowered while being rotated to be spirally cut with a tool 4, as depicted in Figure 10 under the test environment and cutting conditions below. At this time, the cutting resistance of the work material was measured with a multi-component force dynamometer (9129AA, manufactured by Kistler Group). The results are presented in Table 1.

(Test Environment)

25 [0054]

30

35

40

45

50

55

10

Machine used: NV5000α 1B/40 (manufactured by DMG MORI Co., Ltd.)

Holder 1: BBT40-HMC25S-75 (manufactured by BIG Daishowa Seiki Co., Ltd.)

Holder 2: ST14-MEGA6S-160 (manufactured by BIG Daishowa Seiki Co., Ltd.)

Tool bit: MVLNR2525M-16 (manufactured by KYOCERA Corporation)

Lubricant: YUSHIROKEN FGE 234 (manufactured by Yushiro Chemical Industry Co., Ltd., from 5 to 10% concen-

tration)

(Cutting Conditions)

Cutting speed: 40 m/min

Feed rate per revolution: 0.01 mm/rev

Depth of cut into copper alloy: 0.25 mm (2 passes)

[Table 1]

5			Swarf profile	Undulatory	Undulatory	Undulatory	Slightly sheared	Slightly sheared	Sheared	Sheared
10		Machinability	Degree of unevenness of swarf h <sub>2</sub> /h <sub>1</sub>	1.03	1.05	1.11	2.11	2.93	6.51	09.9
15		Table 1  Co-Be-Si intermetallic compound grains	Cutting resistance (N)	6.44	76.7	6.42	6.38	6.45	6.34	69'9
20			Cross sectional area per grain (μm²)	ı	ı	0.2	0.3	4.2	7.3	6.69
25			Number of grains per 1 mm² at copper alloy cross section	ı	ı	48	62	85	104	311
30	Table 1		Hardness (GPa)	ı	ı	from 1.0 to 12	from 1.0 to 12	from 1.0 to 12	from 1.0 to 12	from 1.0 to 12
35			Cu	Balance	Balance	Balance	Balance	Balance	Balance	Balance
40		er alloy (wt%)	Pb	0.39	1	1	-	-	-	-
		u copp	- F	0.15	0.04	0.02	0.03	0.02	0.02	0.03
45		Composition of beryllium copper alloy	Ë	0.01	0.01	<0.01	0.01	<0.01	0.01	0.01
		sition of	S	0.21	0.24	0.24	0.23	0.25	0.25	0.25
50		Compos	: <u>S</u>	-	ı	0.18	0.29	0.47	1.09	2.98
			Be	1.92	1.95	2.11	1.83	1.91	2.05	1.98
55	[0055]			Example 1*	Example 2*	Example 3*	Example 4	Example 5	Example 6	Example 7

Asterisk \* represents Comparative Example.

[0056] The results in Table 1 show that allowing beryllium copper alloys to contain Si improved machinability in terms of reduced cutting resistance, improved swarf shape, reduced surface roughness of work materials, and improved tool life. In other words, the lower the cutting resistance of beryllium copper alloy, the better the machinability, and allowing the beryllium copper alloy to contain Si reduced the cutting resistance more than Si-free beryllium copper alloys and provided machinability equivalent to Pb-containing beryllium copper alloys. Also, reduced cutting resistance probably leads to improved tool life. Furthermore, allowing beryllium copper alloys to contain Si enables the swarf cross section to have a more sheared profile with zigzag-shaped unevenness than Si-free beryllium copper alloys, resulting in desired swarf shapes.

10 <EBSD Measurement of Area Percentage of BCC Region>

[0057] Copper alloy samples of Examples 1 and 5 to 7 were cut and subjected to Ar ion milling to obtain cross sections to be measured. The area percentage of BCC phases was measured by EBSD with a scanning electron microscope (FE-SEM, JSM-7800F manufactured by JEOL Ltd.) and an OIM crystal orientation analyzer (OIM Data Collection / OIM, manufactured by TSL Solutions K. K.). This EBSD measurement was conducted under the conditions of 15 kV accelerating voltage and  $0.2~\mu m$  step size.

[0058] As a result, SEM images presented in Figure 11 and the EBSD phase maps in the regions corresponding to their images were obtained. That is, Figure 11 presents EBSD phase maps in the region surrounded by the frame in each SEM image. In the EBSD phase maps, the FCC regions identified as face-centered cubic (FCC) lattices and the BCC regions identified as body-centered cubic (BCC) lattices are represented in different color tones. Then, in the resulting EBSD phase maps, the percentage of area  $S_{BCC}$  of the BCC regions to the total area of area  $S_{FCC}$  of the FCC regions and area  $S_{BCC}$  of the BCC regions (that is,  $100 \times S_{BCC}$  / ( $S_{FCC} + S_{BCC}$ )) was calculated to obtain the values presented in Table 2 (see Figure 11). In addition, Table 2 (see Figure 11) also presents cutting resistances (thrust forces). The results presented in Table 2 (see Figure 11) reveal that the area percentage of BCC phases (that is, Si-rich phases) increases with increasing amount of Si added and that the cutting resistance (particularly thrust force) decreases (that is, machinability improves) with increasing BCC phase area percentage.

#### Claims

1. A lead-free free-cutting beryllium copper alloy, consisting of:

from 1.80% to 2.10% by weight of Be; from 0.10% to 3.00% by weight of Si; from 0.20% to 0.40% by weight of Co; from 0% to 0.10% by weight of Fe; from 0% to 0.10% by weight of Ni; and the balance being Cu and inevitable impurities, wherein the beryllium copper alloy has:

40

15

20

30

35

a matrix phase being an  $\alpha$  phase,

a Si-rich phase being a  $\kappa$  phase rich in Si, and

Co-Be-Si intermetallic compound grains containing Co, Be, and Si, and optionally Fe and/or Ni.

- **2.** The lead-free free-cutting beryllium copper alloy according to claim 1, wherein the Co-Be-Si intermetallic compound grains exhibit a hardness from 1.0 to 12.0 GPa as measured by a nanoindentation test in accordance with ISO14577.
  - **3.** The lead-free free-cutting beryllium copper alloy according to claim 1 or 2, wherein the number of the Co-Be-Si intermetallic compound grains present at a cross section of the lead-free free-cutting beryllium copper alloy is 320 or less per unit area of 1 mm<sup>2</sup>.
  - 4. The lead-free free-cutting beryllium copper alloy according to claim 1 or 2, wherein when a cross section of the lead-free free-cutting beryllium copper alloy is observed, the Co-Be-Si intermetallic compound grains have a cross-sectional area from 0.3 to 70  $\mu$ m<sup>2</sup> per grain.

55

50

**5.** The lead-free free-cutting beryllium copper alloy according to claim 1 or 2, wherein when a cross section of swarf generated by cutting the lead-free free-cutting beryllium copper alloy is observed along a longitudinal direction, the cross section of the swarf has a sheared profile with zigzag-shaped unevenness that satisfies a relationship 1.10 <

 $h_2/h_1 < 6.60$ , wherein  $h_1$  represents the average of distances between recesses in the zigzag-shaped unevenness, and  $h_2$  represents the average of heights of protrusions in the unevenness.

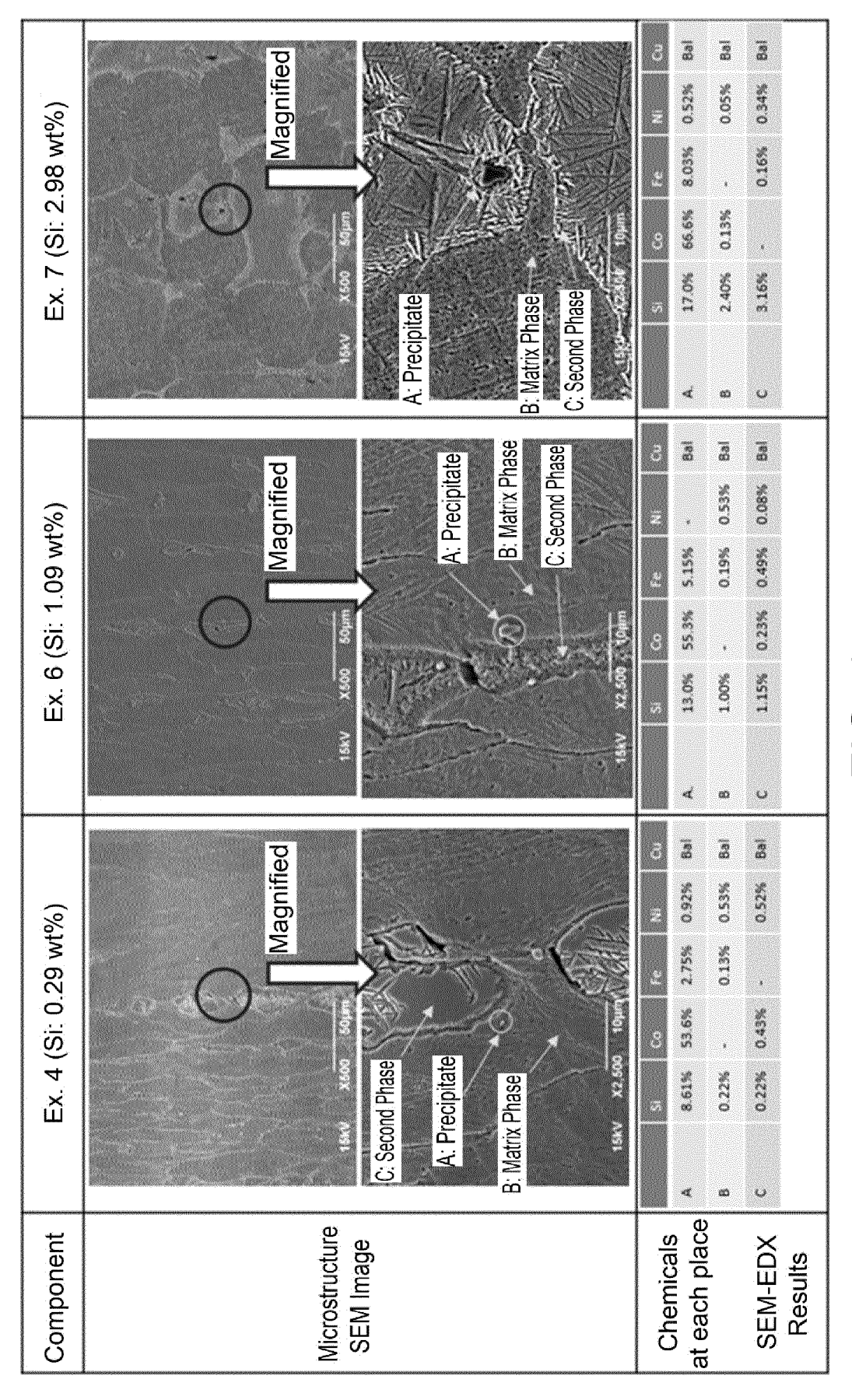
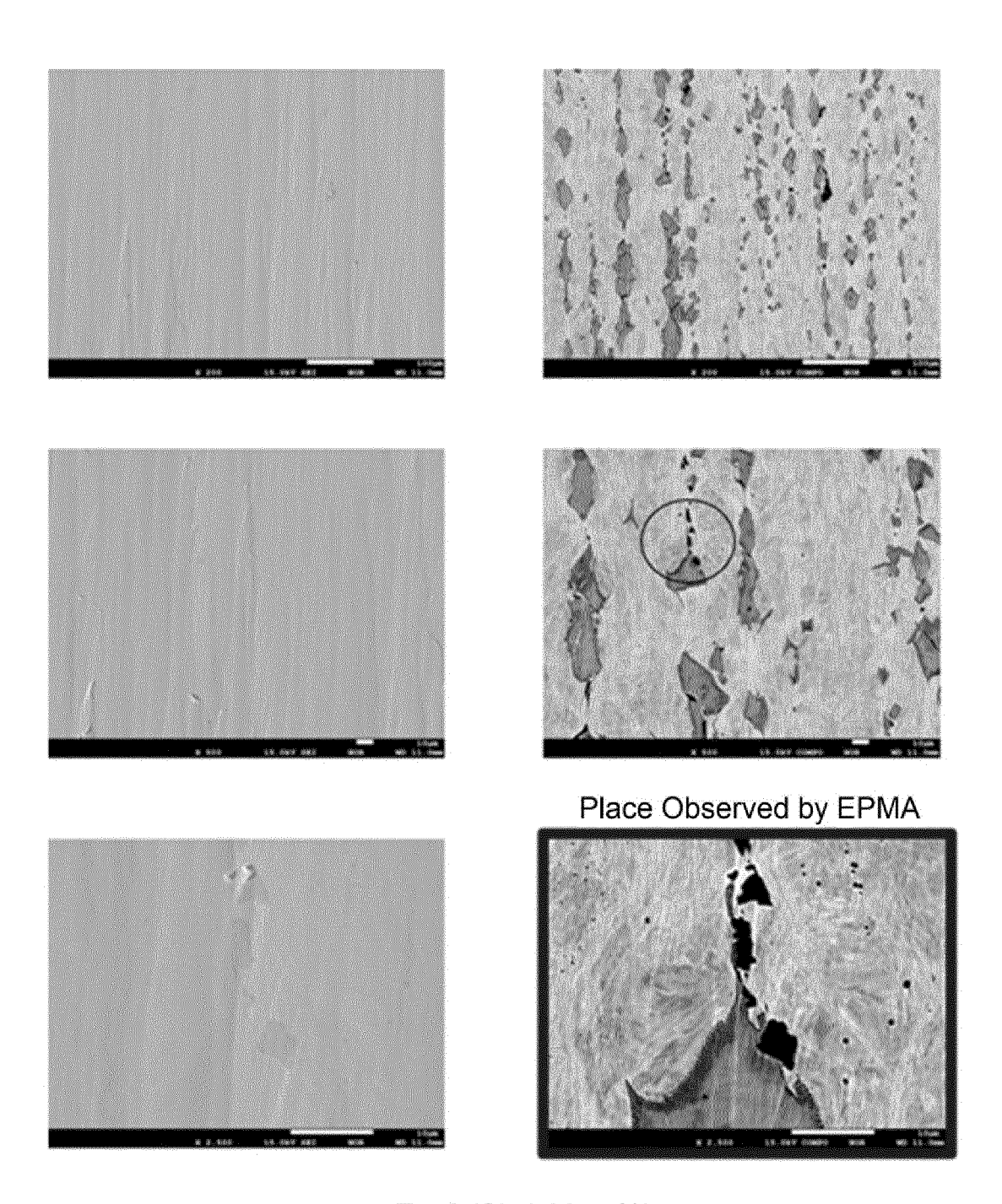
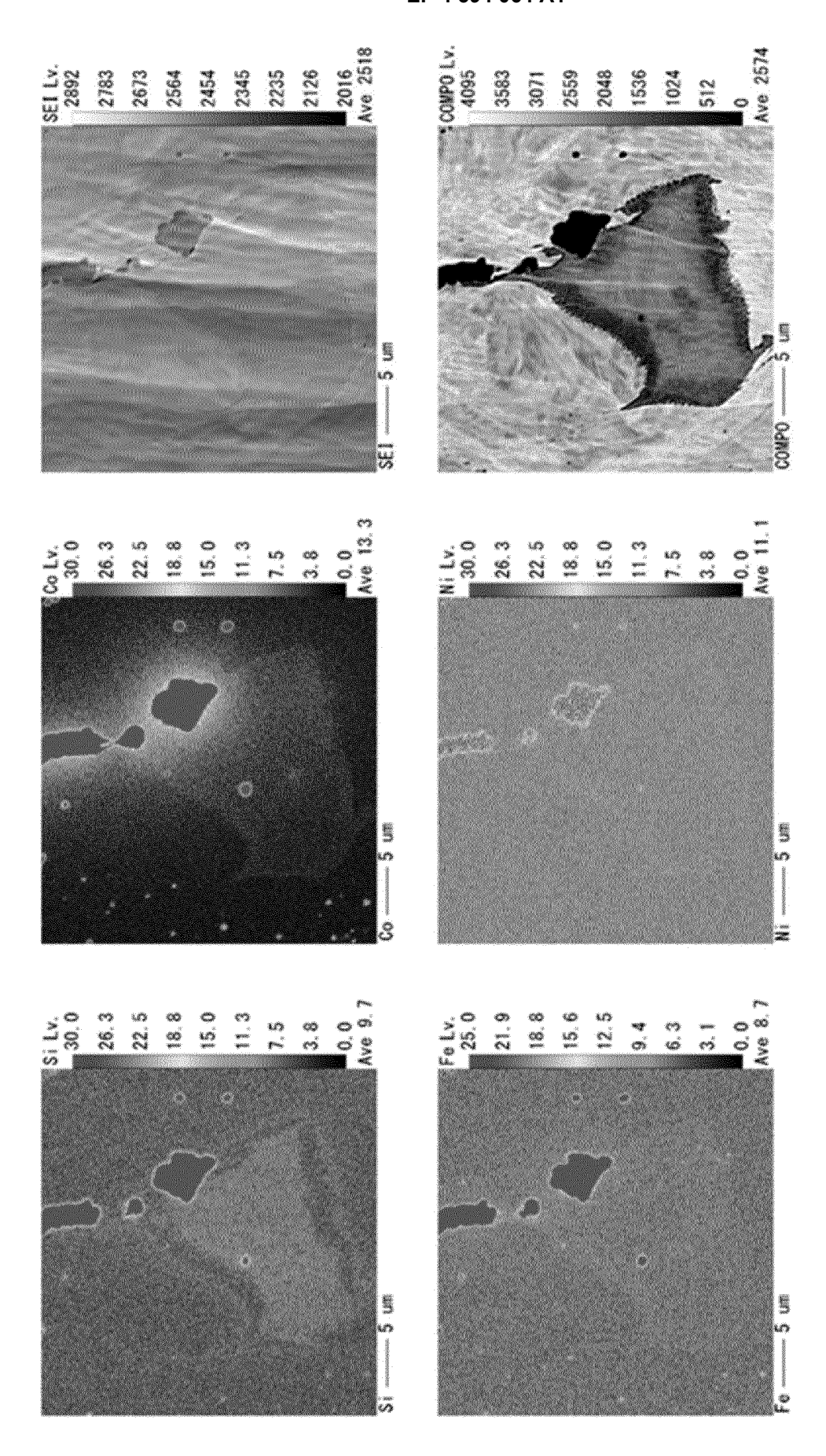


FIG. 1

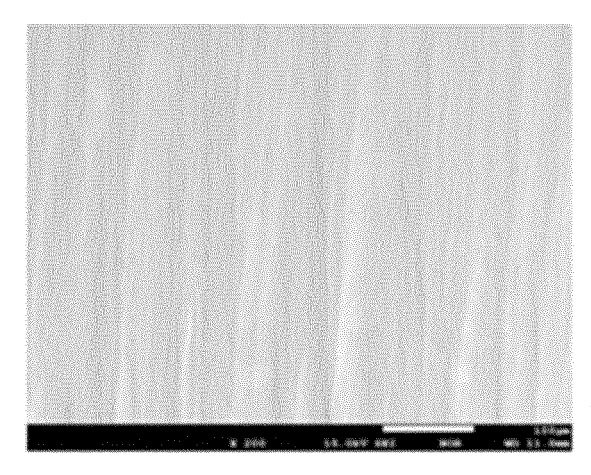


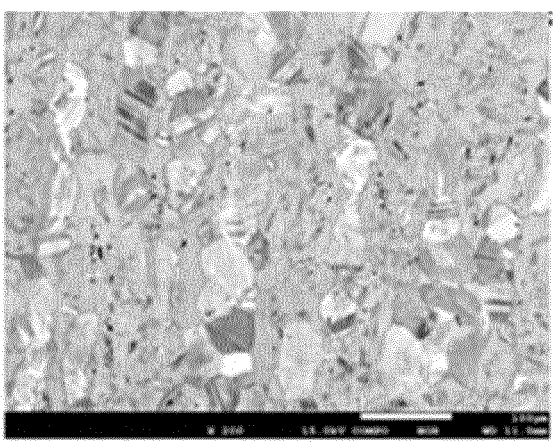
Ex. 6 (Si: 1.09 wt%)

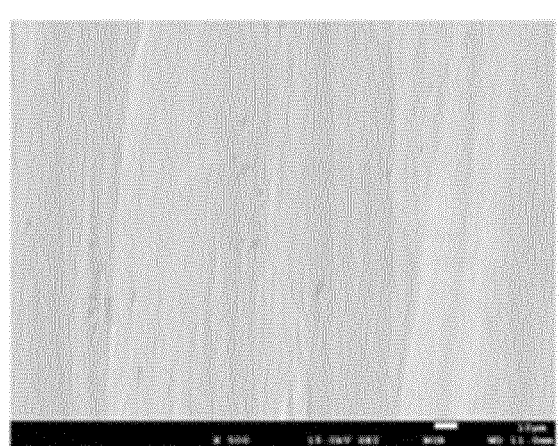
FIG. 2A

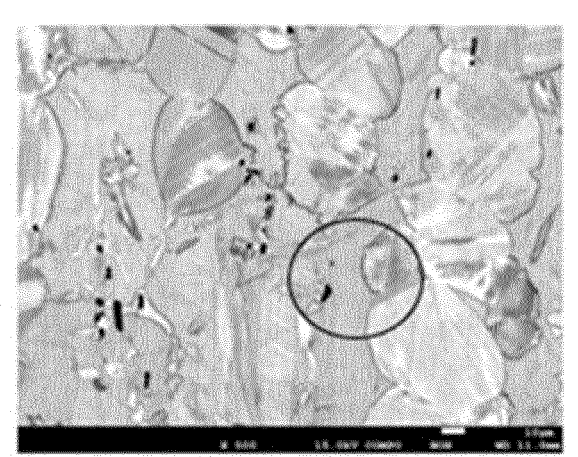


Ex. 6 (Si: 1.09 wt%) FIG. 2B

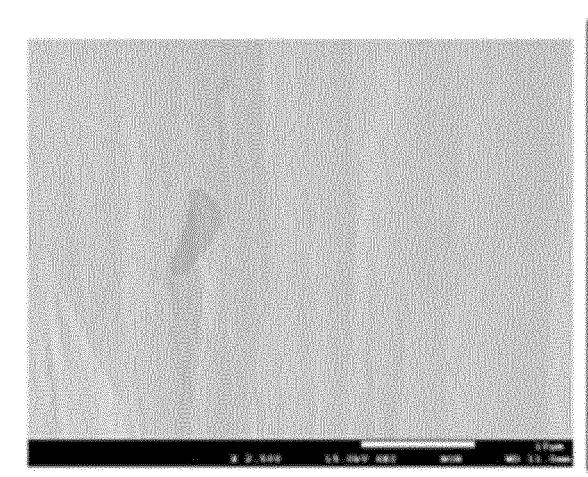


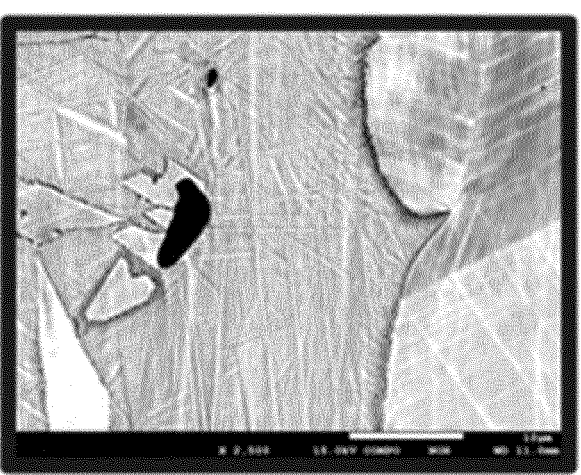






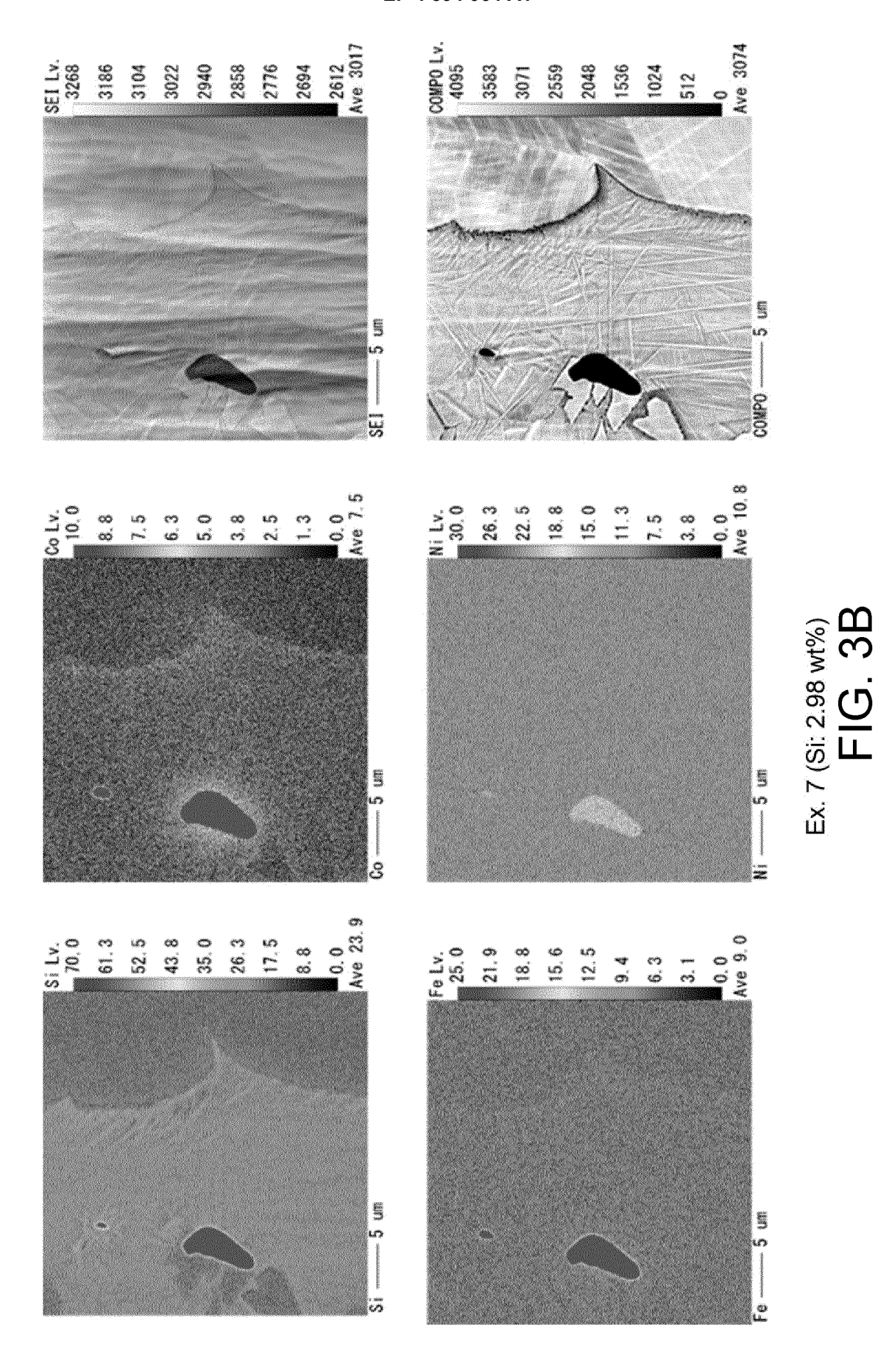
Place Observed By EPMA

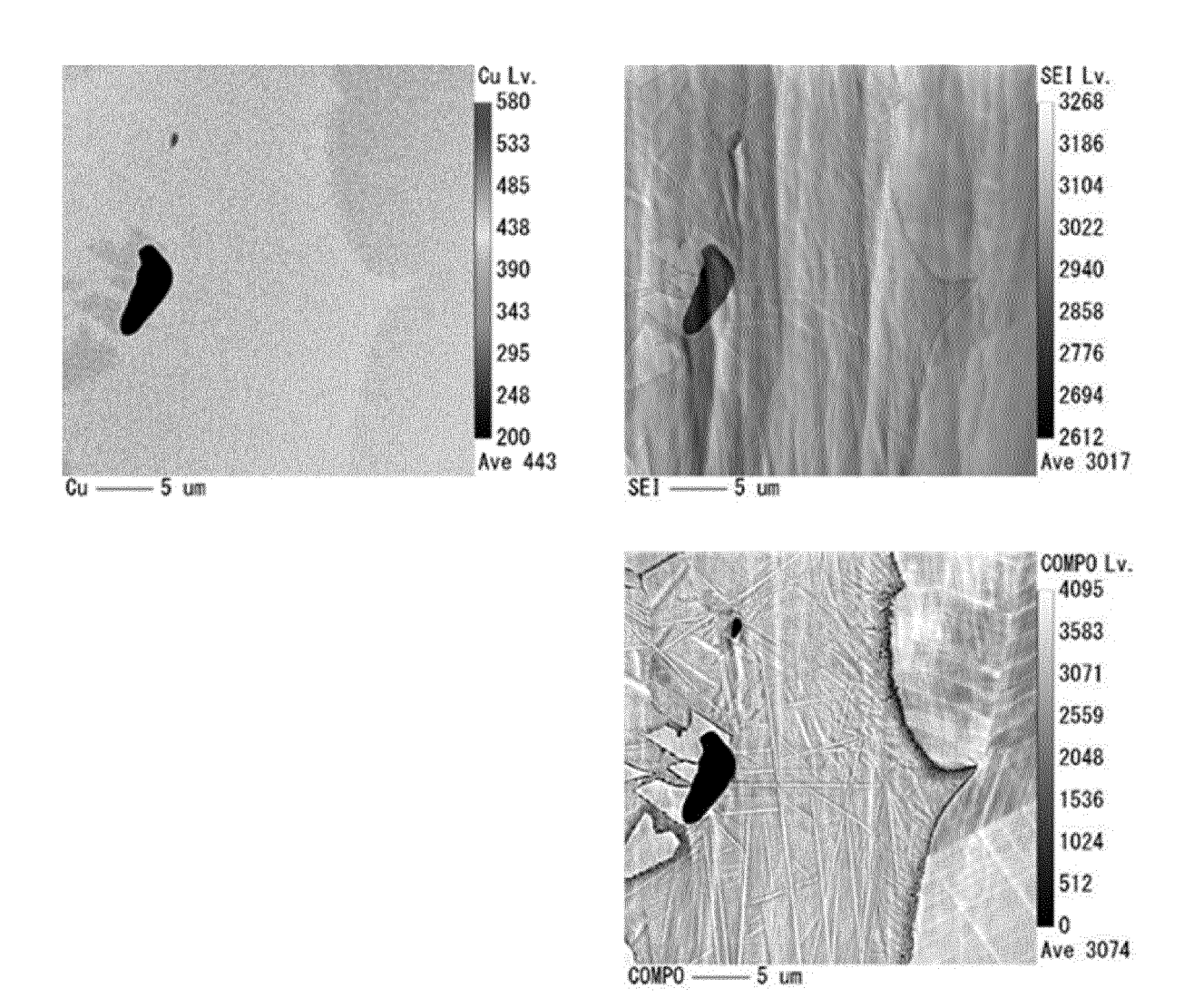




Ex. 7 (Si: 2.98 wt%)

FIG. 3A





Ex. 7 (Si: 2.98 wt%)

FIG. 3C

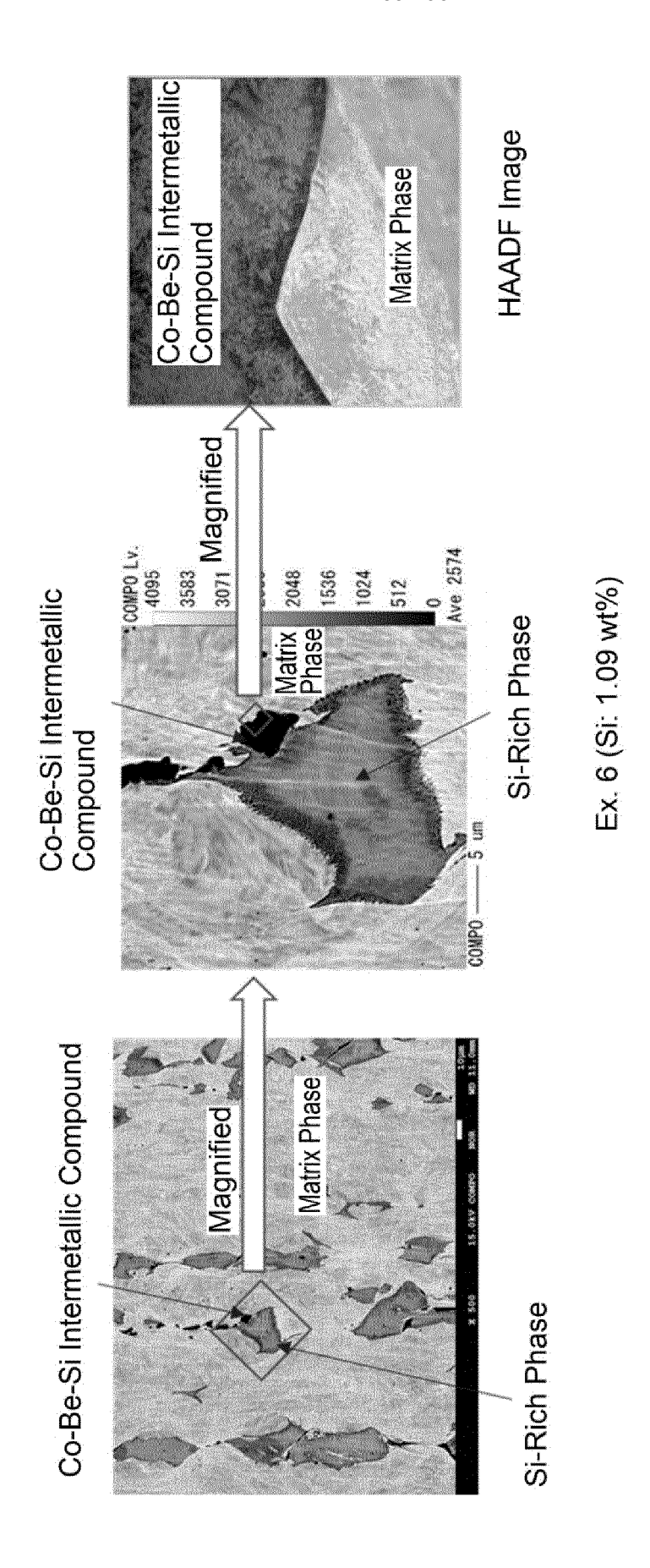
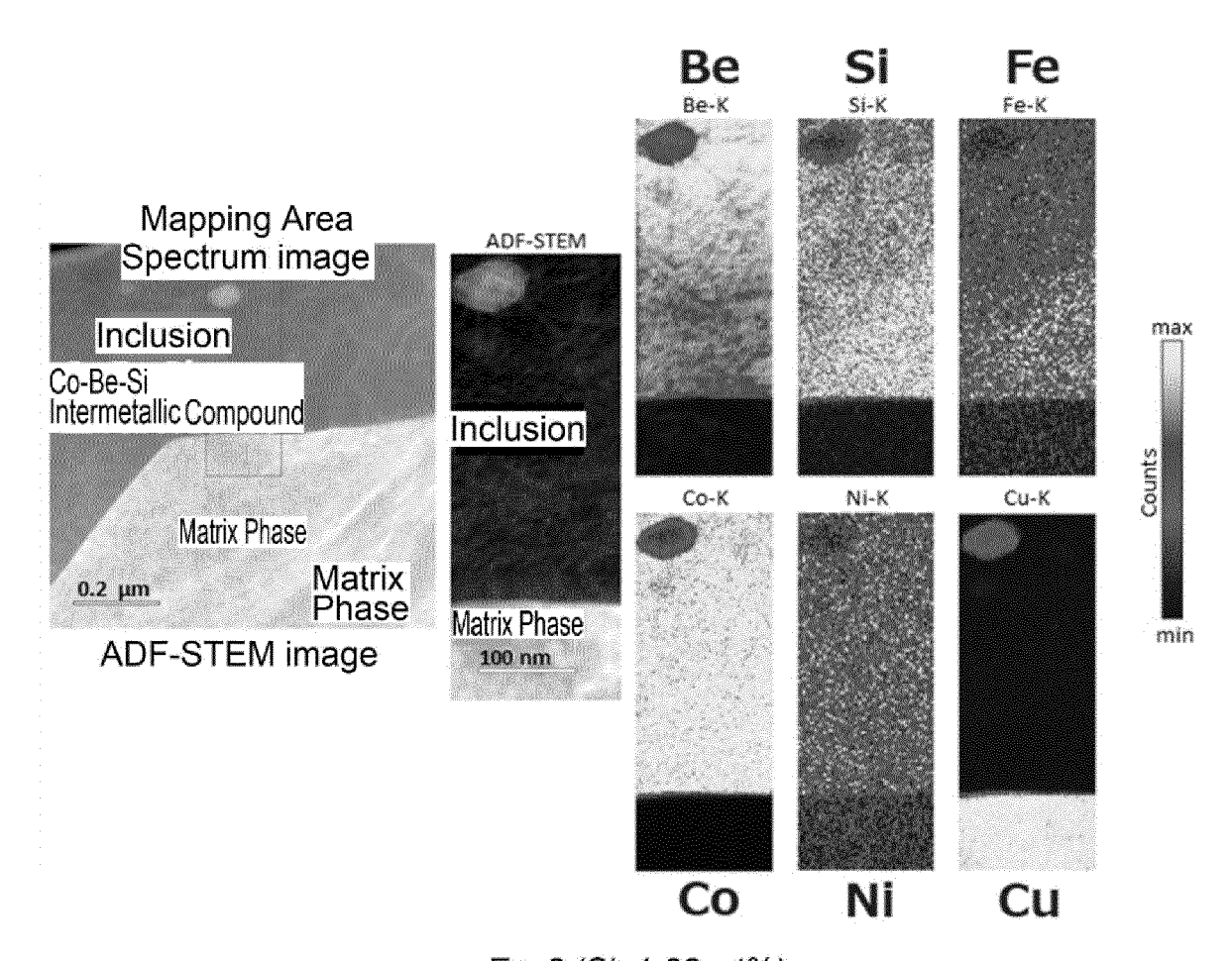
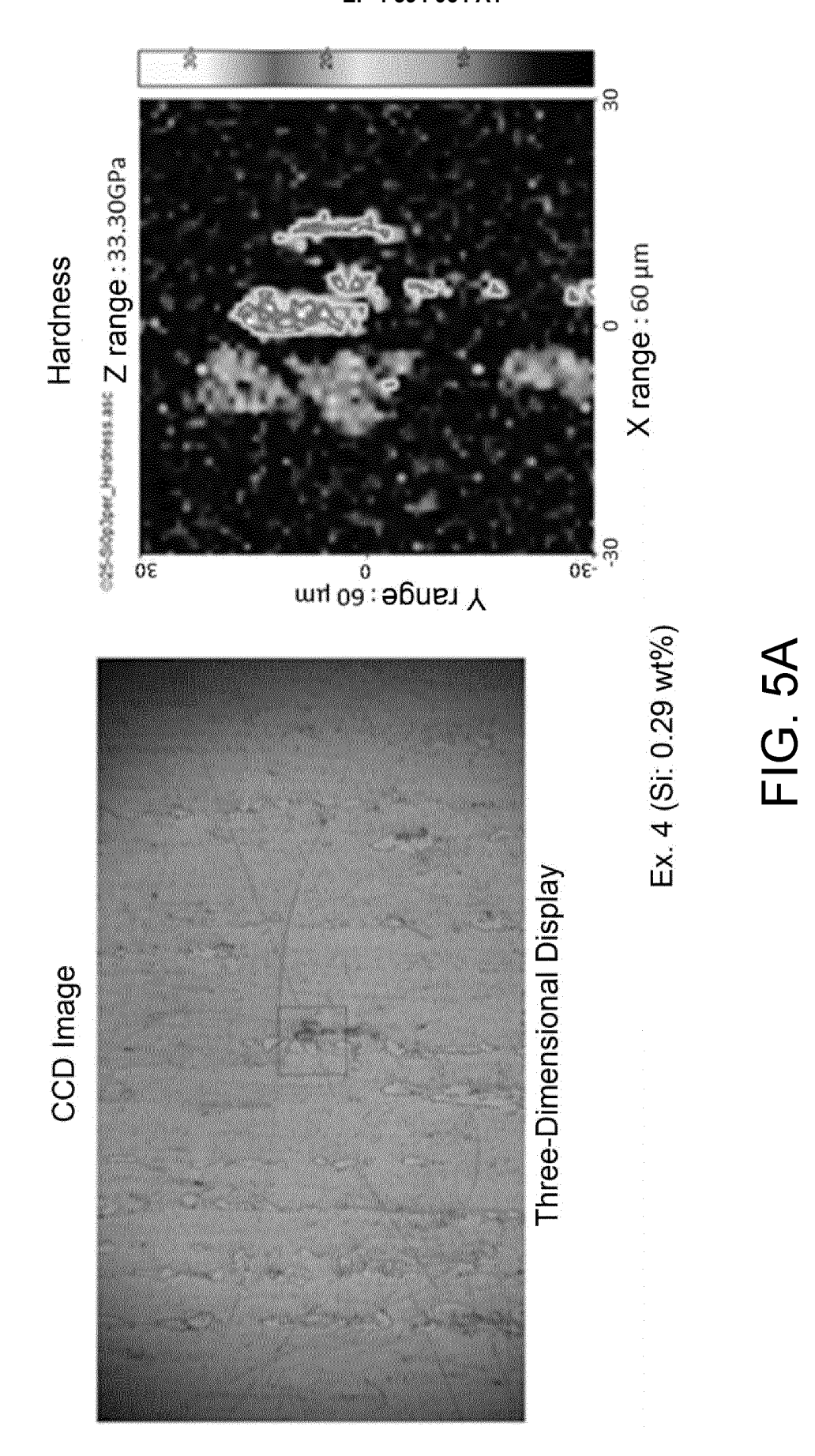


FIG. 4A

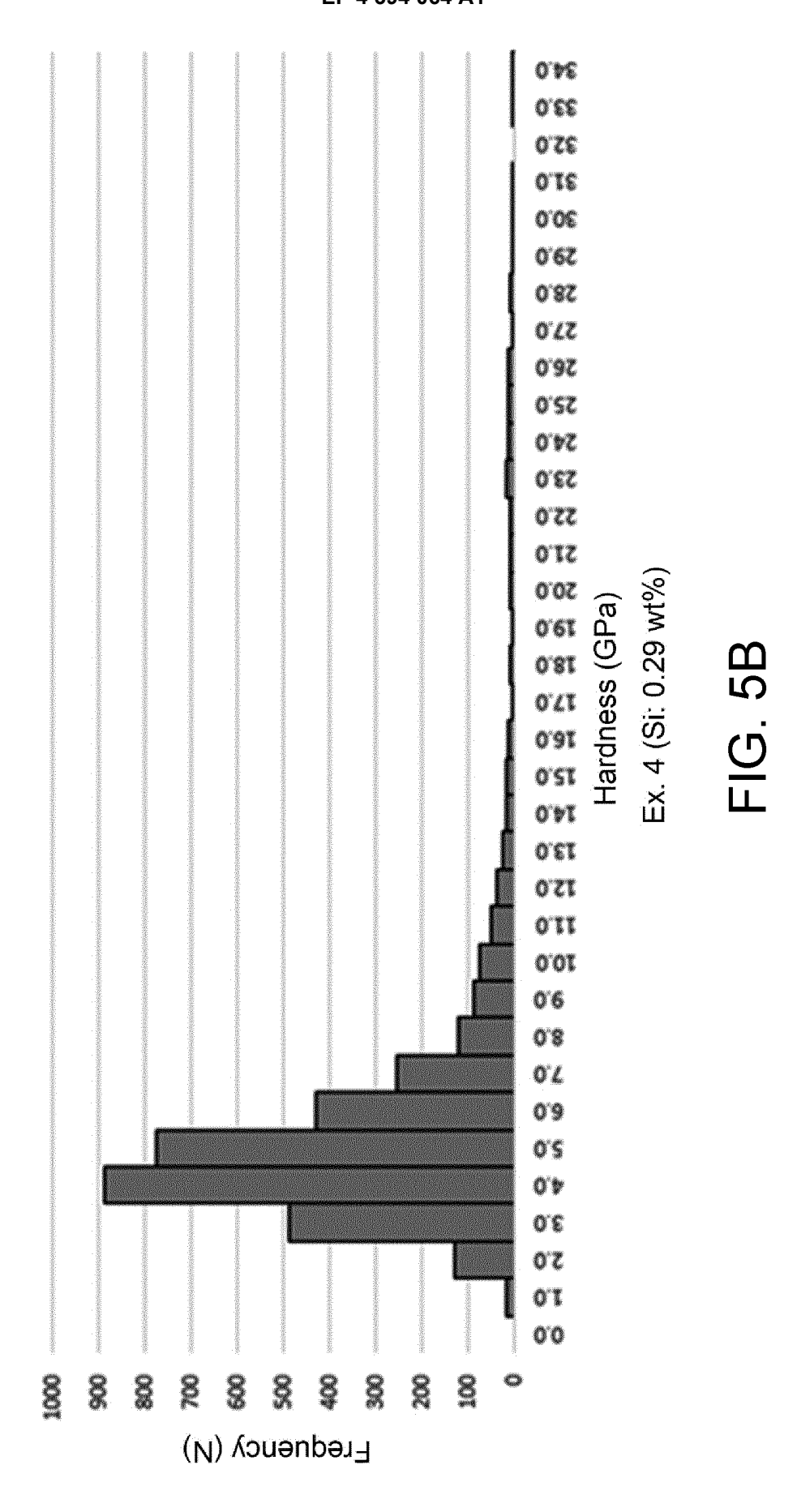


Ex. 6 (Si: 1.09 wt%)

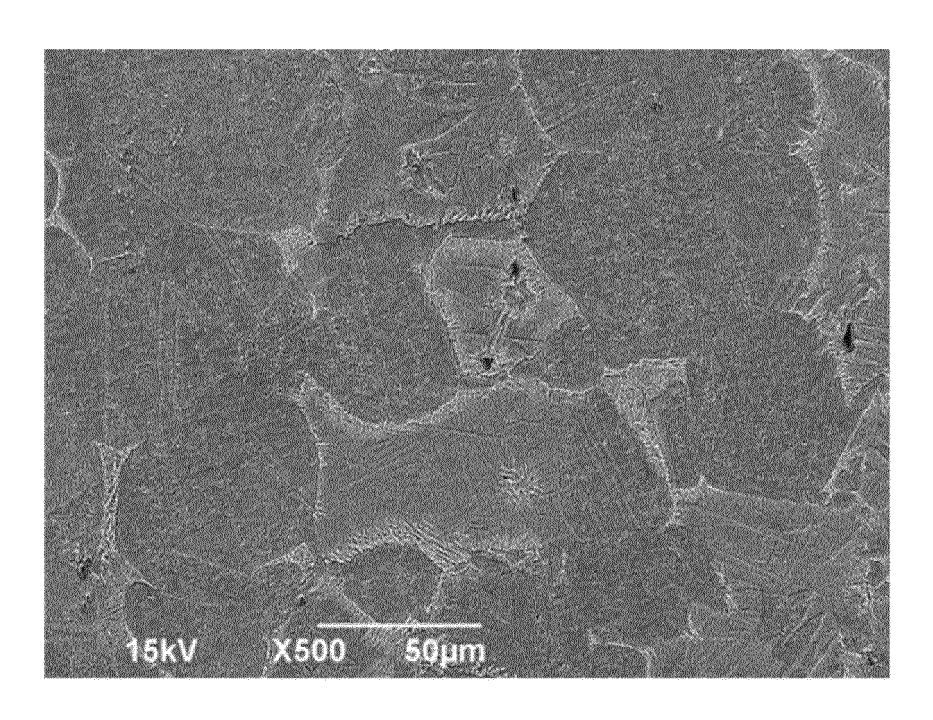
FIG. 4B



21

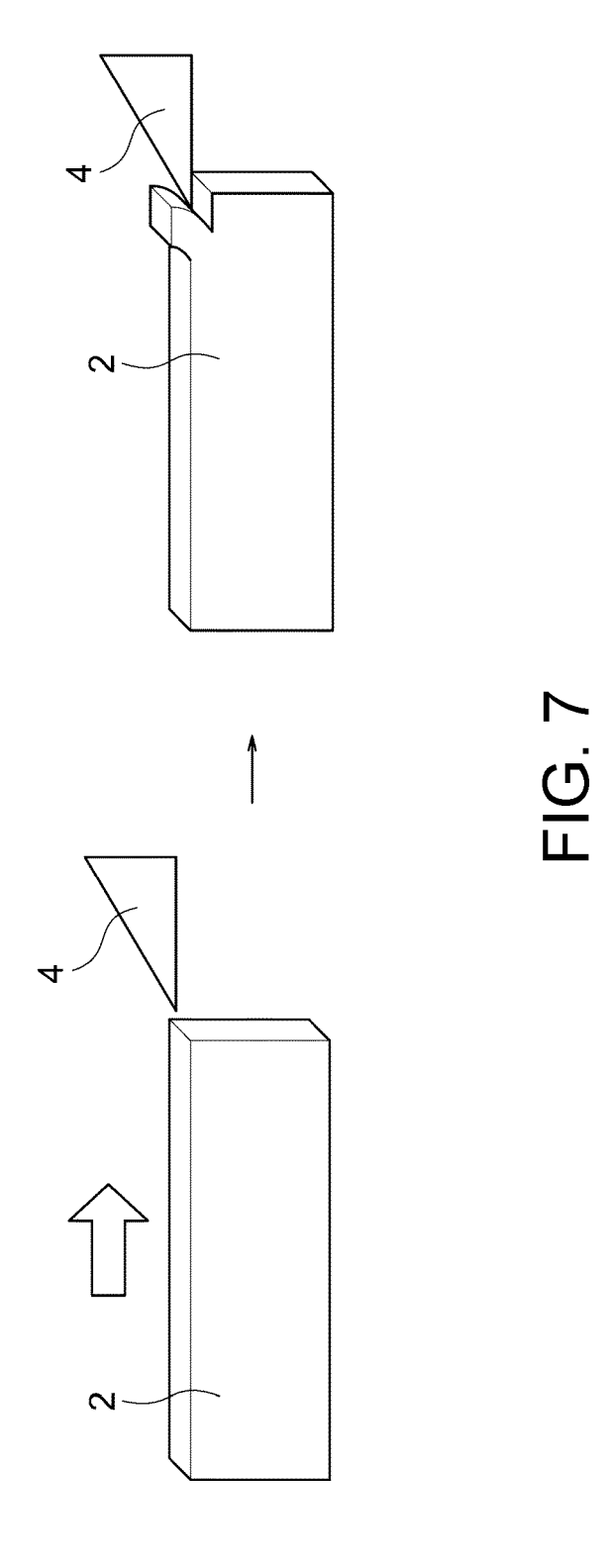


22



Ex. 7 (Si: 2.98 wt%)

FIG. 6



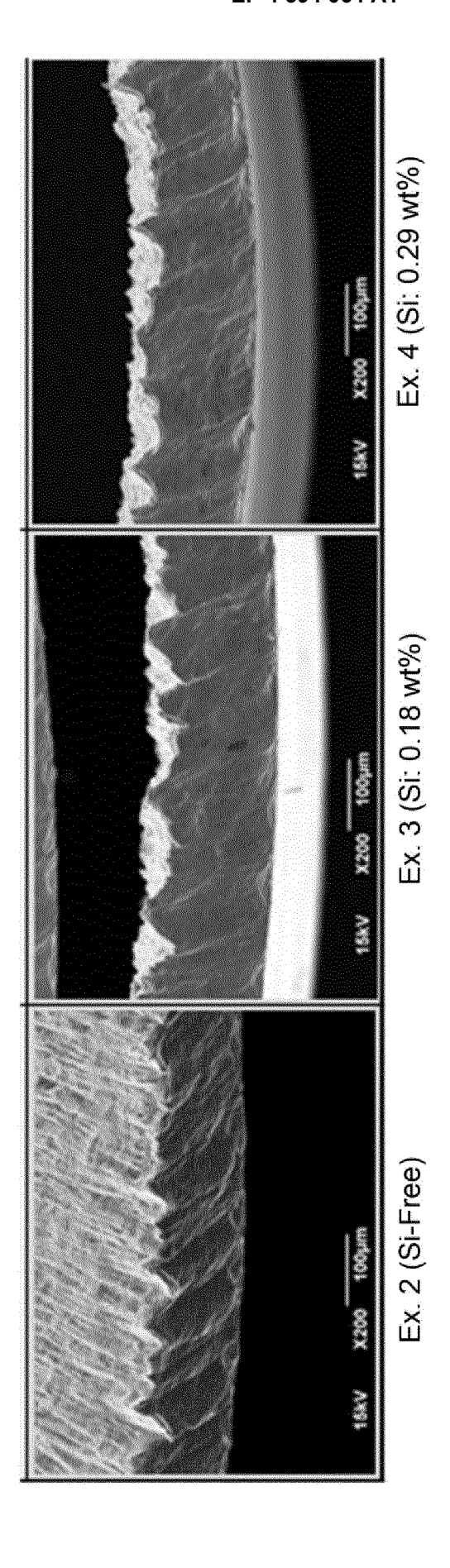


FIG. 8A

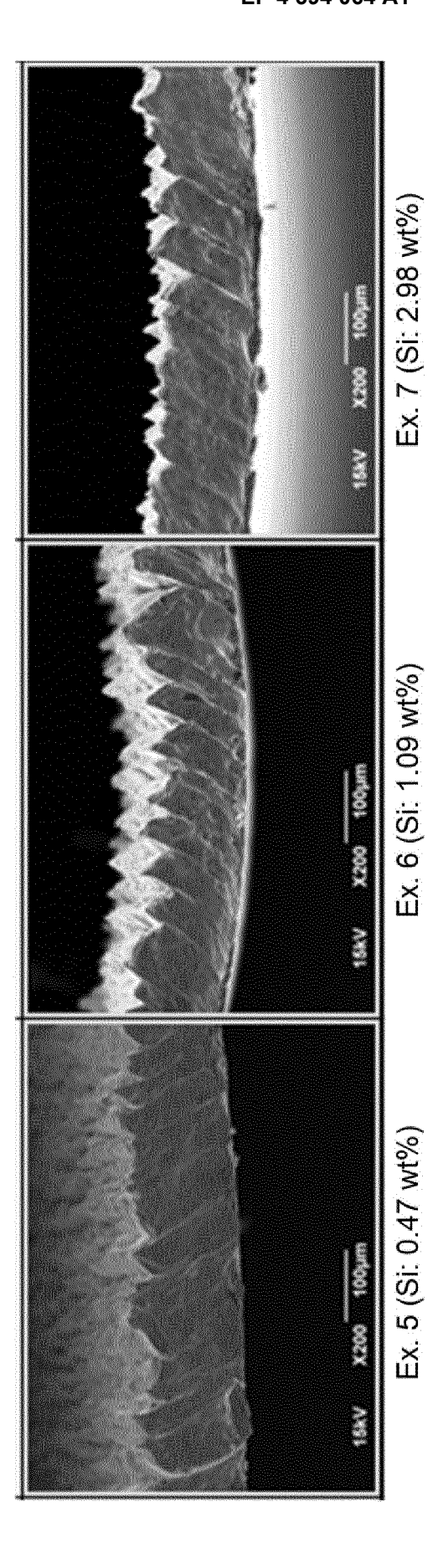


FIG. 8B

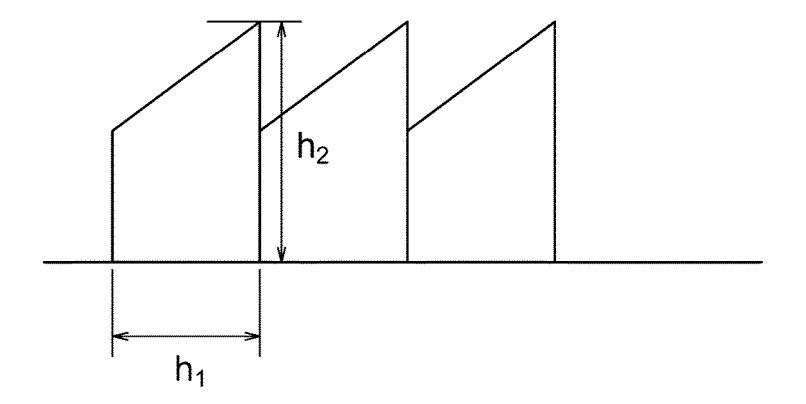


FIG. 9

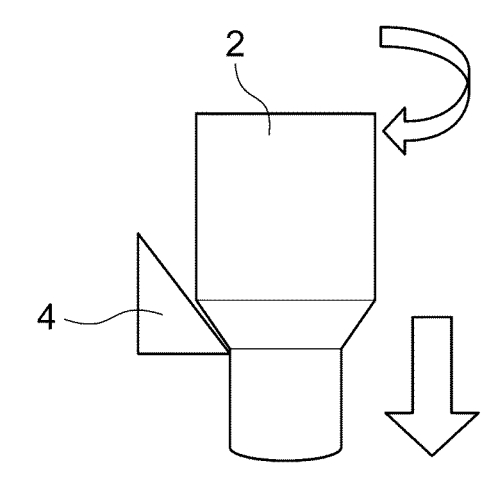


FIG. 10

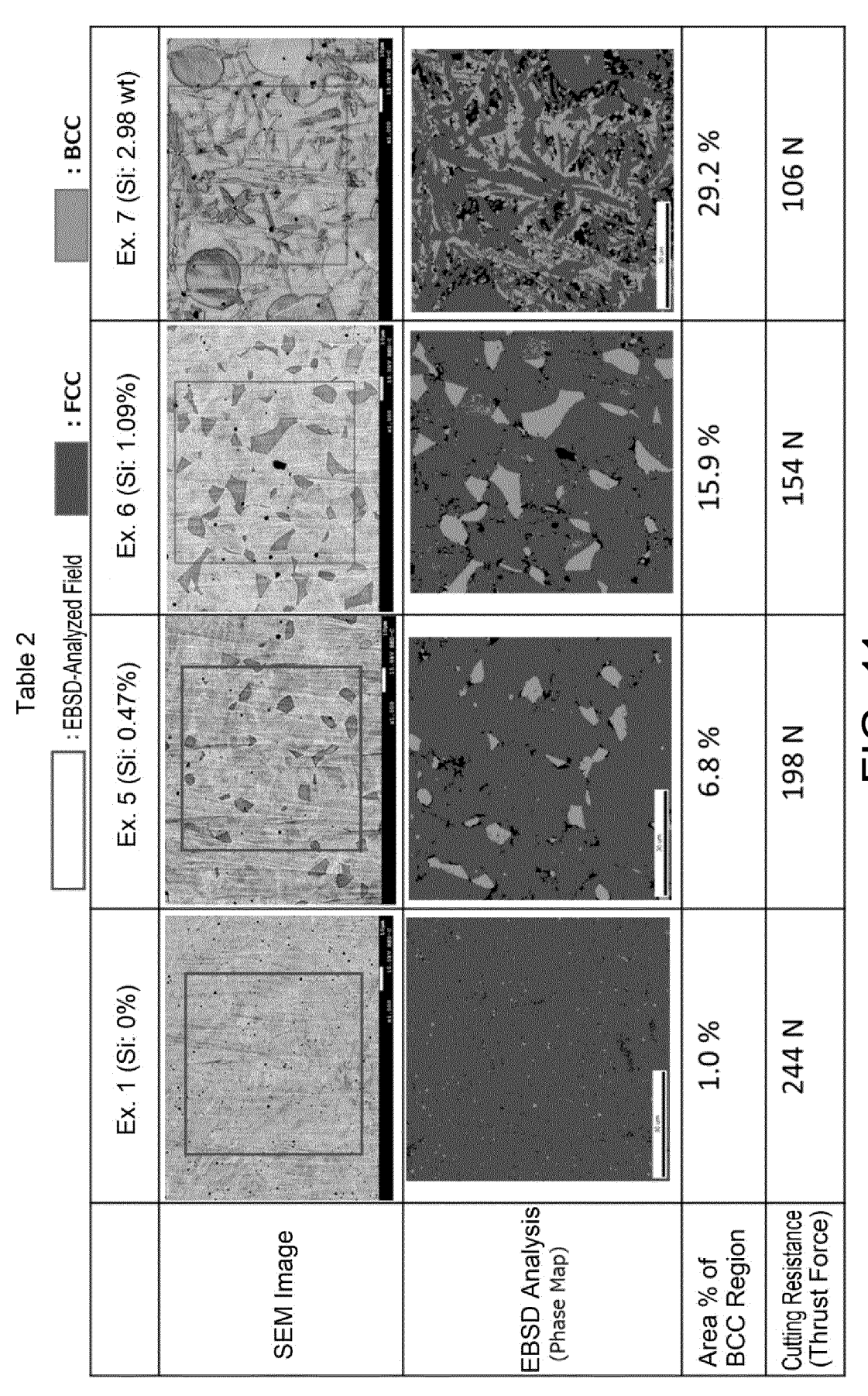


FIG. 11

#### INTERNATIONAL SEARCH REPORT

International application No.

PCT/JP2023/032138

5

10

15

20

25

30

35

40

45

CLASSIFICATION OF SUBJECT MATTER

 $\textbf{\textit{C22C 9/00}} (2006.01) \text{i; } \textbf{\textit{C22C 9/10}} (2006.01) \text{i; } \textbf{\textit{C22F 1/00}} (2006.01) \text{i; } \textbf{\textit{C22F 1/08}} (2006.01) \text{i}$ 

C22C9/00; C22C9/10; C22F1/00 602; C22F1/00 624; C22F1/00 630A; C22F1/00 630G; C22F1/00 630J; C22F1/00 630K; C22F1/00 640A; C22F1/00 650A; C22F1/00 681; C22F1/00 682; C22F1/00 683; C22F1/00 684B; C22F1/00 684C; C22F1/00 685Z; C22F1/00 686B; C22F1/00 691B; C22F1/00 691C; C22F1/00 694A; C22F1/00 694B; C22F1/08

According to International Patent Classification (IPC) or to both national classification and IPC

#### FIELDS SEARCHED

Minimum documentation searched (classification system followed by classification symbols)

C22C9/00; C22C9/10; C22F1/00; C22F1/08

Documentation searched other than minimum documentation to the extent that such documents are included in the fields searched

Published examined utility model applications of Japan 1922-1996

Published unexamined utility model applications of Japan 1971-2023

Registered utility model specifications of Japan 1996-2023

Published registered utility model applications of Japan 1994-2023

Electronic data base consulted during the international search (name of data base and, where practicable, search terms used)

#### DOCUMENTS CONSIDERED TO BE RELEVANT

Category*	Citation of document, with indication, where appropriate, of the relevant passages	Relevant to claim No.
A	JP 2008-297617 A (DOWA METALTECH K.K.) 11 December 2008 (2008-12-11) entire text	1–6
A	JP 9-263859 A (NGK INSULATORS LTD.) 07 October 1997 (1997-10-07) entire text	1–6
A	JP 63-143247 A (NGK INSULATORS LTD.) 15 June 1988 (1988-06-15) entire text	1–6
A	JP 63-125648 A (NGK INSULATORS LTD.) 28 May 1988 (1988-05-28) entire text	1-6

Special categories of cited documents:

See patent family annex.

document defining the general state of the art which is not considered to be of particular relevance "E"

Further documents are listed in the continuation of Box C.

- to be of particular relevance earlier application or patent but published on or after the international filing date document which may throw doubts on priority claim(s) or which is cited to establish the publication date of another citation or other special reason (as specified) document referring to an oral disclosure, use, exhibition or other
- document published prior to the international filing date but later than the priority date claimed

**04 October 2023** 

- later document published after the international filing date or priority date and not in conflict with the application but cited to understand the principle or theory underlying the invention document of particular relevance; the claimed invention cannot be considered novel or cannot be considered to involve an inventive step when the document is taken alone
- document of particular relevance; the claimed invention cannot be considered to involve an inventive step when the document is combined with one or more other such documents, such combination being obvious to a person skilled in the art

17 October 2023

document member of the same patent family

Date of mailing of the international search report

50

Name and mailing address of the ISA/JP Japan Patent Office (ISA/JP)

3-4-3 Kasumigaseki, Chiyoda-ku, Tokyo 100-8915 Japan

Date of the actual completion of the international search

Authorized officer

Telephone No

Form PCT/ISA/210 (second sheet) (January 2015)

55

# INTERNATIONAL SEARCH REPORT International application No. Information on patent family members PCT/JP2023/032138 5 Patent document cited in search report Publication date Publication date (day/month/year) Patent family member(s) (day/month/year) 2008-297617 11 December 2008 (Family: none) JР 9-263859 07 October 1997 (Family: none) 10 15 June 1988 JP 63-143247 (Family: none) JP 4792365 63-125648 28 May 1988 US A Α entire text 271991 EP A2 DE 3773470 A KR 10-1988-0006721 15 20 25 30 35 40 45 50

55

Form PCT/ISA/210 (patent family annex) (January 2015)

#### REFERENCES CITED IN THE DESCRIPTION

This list of references cited by the applicant is for the reader's convenience only. It does not form part of the European patent document. Even though great care has been taken in compiling the references, errors or omissions cannot be excluded and the EPO disclaims all liability in this regard.

## Patent documents cited in the description

- JP S50139017 A [0002] [0005]
- JP S5430369 B **[0003] [0005]**

- JP 2000119775 A [0004] [0005]
- JP 2021042459 A [0004] [0005]